Structural characterization of laser-treated Cr_3C_2–NiCr coatings

P. Serra
Universitat de Barcelona, Departament de Física Aplicada i Òptica, Av. Diagonal 647, E-08028 Barcelona, Spain

J.M. Miguel
Universitat de Barcelona, Departament d'Enginyeria Química i Metal.lúrgia, Av. Diagonal 647, E-08028 Barcelona, Spain

J.L. Morenza
Universitat de Barcelona, Departament de Física Aplicada i Òptica, Av. Diagonal 647, E-08028 Barcelona, Spain

J.M. Guilemany
Universitat de Barcelona, Departament d'Enginyeria Química i Metal.lúrgia, Av. Diagonal 647, E-08028 Barcelona, Spain

(Received 26 February 2001; accepted 10 September 2001)

The interconnected porosity of the Cr_3C_2–NiCr coatings obtained by high-velocity oxy fuel spraying is detrimental in corrosion and wear resistance applications. Laser treatments allow sealing of their surfaces through melting and resolidification of a thin superficial layer. A Nd:YAG laser beam was used to irradiate Cr_3C_2–NiCr coatings either in the continuous wave mode or at different repetition rates in the pulsed one. Results indicated that high peak and low mean laser irradiances are not good, since samples presented deep grooves and an extensive crack network. At low peak and higher mean laser irradiances the surface was molten, and only a few shallow cracks were observed. The interconnected porosity was completely eliminated in a layer up to 80 μm thick, formed by large Cr_7C_3 grains imbedded in a NiCr matrix.

I. INTRODUCTION

Both the high wear and corrosion resistance at high temperatures of Cr_3C_2 and NiCr, respectively, make ceramic–metal Cr_3C_2–NiCr composite coatings especially adequate to protect steel in many industrial applications. The high velocity oxy fuel spraying (HVOF) technique has been revealed as an appropriate method for obtaining good adherent coatings of this composite on steel.[1–6] Unfortunately, they present a high amount of interconnected porosity, which is detrimental to corrosion resistance since it provides channels of penetration for the aggressive agents to reach the substrate. One way to overcome this problem is to seal the coating's surfaces through melting and resolidification by means of laser irradiation. This process leads not only to the total elimination of the superficial porosity but also induces changes in the morphology and composition of the coatings that can enhance their wear resistance, as has already been observed in this material[7] and many others.[8–14] Although most of the treatments have been carried out with continuous wave (CW) lasers, some authors[10,15] have suggested the convenience of working in the pulsed mode since it would reduce the extent of the heat-affected zone beyond the layer molten by the laser beam and thus protect the bulk of the coating and the substrate from alteration. This has motivated us to undertake a study analyzing the differences between both CW and pulsed laser irradiation regimes to determine the conditions where the laser surface treatment is more effective.

In this paper we present the results obtained after Nd:YAG laser surface treatment of Cr_3C_2–NiCr coatings in both CW and pulsed irradiation modes. The samples as obtained were characterized through different techniques that allowed us to analyze the effect of the laser repetition rate on the changes induced in the material and to clarify which processes are responsible for these changes.

II. EXPERIMENTAL

A HVOF gun (Plasma Technik CDS-100, Switzerland) was used to spray an AMDRY 5260 (Sulzer Metco) Cr_3C_2–NiCr powder (75% carbide and 25% metallic phase) onto steel substrates leading to the formation of 300-μm-thick coatings. The powder consisted of spheroidal −45 +11 μm particles, obtained by agglomeration and densification. A mixture of oxygen, propylene, and

nitrogen carrier gas was set at fluxes of 420, 60, and 25 l/min, respectively. The distance between the gun exit and the substrate was 300 mm.[1]

Laser surface treatments were performed with a Nd:YAG marking laser, 1.064-μm wavelength, that can operate either in CW or pulsed mode. Table I summarizes the main characteristics of the laser output at the different operation modes and the different repetition rates explored in this work with constant pumping lamp current. It is important to note that the beam parameters cannot be independently controlled: as the repetition rate increases, the pulse energy decreases and the pulse duration increases. It means that increasing the repetition rate necessarily leads to deliver a higher amount of longer and less-energetic laser pulses per unit area and time on the material. The combination of all these effects is summarized in the secondary parameters peak irradiance (pulse energy per unit area divided by pulse duration) and average irradiance (pulse energy per unit area multiplied by repetition rate), the competition between which will account for the way energy is delivered to the material. The samples were placed at a position where the diameter of the laser beam was about 350 μm. This laser is furnished with computer-controlled galvanometric mirrors that deflect the beam and, therefore make it possible to scan a whole area on a stationary sample. Four-millimeter square areas were scanned line by line at a speed of 5 mm/s with a separation between adjacent lines of 100 μm, which results in an overlap of about 70% in area.

The characterizations of both as-sprayed and laser-treated samples were carried out by means of the following techniques: optical and scanning electron microscopy (SEM) to study the morphology of the surface and the cross-sections, x-ray diffractometry (XRD) to determine the crystalline structure, and electron probe microanalysis (EPMA) to analyze the composition of the different compounds present in the coatings.

III. RESULTS

Figure 1(a) depicts a SEM image of the morphology of an as-sprayed coating of Cr_3C_2–NiCr. The morphology of the surface is rough and porous, as is usual in this kind of coating. After laser treatment at a repetition rate of 4 kHz, the morphology changes drastically [Fig. 1(b)]. The image shows the presence of deep horizontal and parallel grooves separated by a distance of about 100 μm, the distance between laser tracks. These structures reveal how the scanning process was performed. The grooves are surrounded by walls of material whose aspect indicates that they were melted and resolidified. Some of this material invades the empty space corresponding to the grooves and builds bridges between adjacent walls. The image also reveals the presence of cracks. Figure 1(c) shows the morphology of the sample surface after laser treatment at 10 kHz. In this case the presence of the laser tracks is also evident, but instead of grooves, there are large holes (about 40 μm in diameter) along these tracks. The aspect of the surface reveals melting and resolidification and there are cracks all over the image. At 30 kHz, the corresponding image [Fig. 1(d)] shows the existence of ridges of resolidified material at the borders of each laser track. There are some small holes and plenty of droplets uniformly spread over the surface of the sample. The presence of some hemispheric protuberances suggests that bubbles formed. No cracks are visible in the image. The image corresponding to irradiation in the CW mode [Fig. 1(e)] is filled with structures that clearly suggest the explosion and further relaxation of bubbles in the melt pool generated by the laser beam. In this case droplets are also present; there are only a very few small holes and it is hard to distinguish the laser tracks. As in the preceeding case, no cracks are visible.

Figure 2 corresponds to optical microscopy images of the cross sections of the more representative samples. The sections were always obtained perpendicular to the laser tracks. In the image corresponding to the untreated sample [Fig. 2(a)], it can be seen that there is an important amount of interconnected porosity covering the whole section of the sample. In addition, it should also be noticed that the surface is rough. Figure 2(b) is an image of the sample treated at a repetition rate of 4 kHz. There are very deep valleys, about 150 μm in depth, separated by distances in multiples of 100 μm, which clearly correspond to the grooves observed in Fig. 1(b). These distances are not always exactly 100 μm, but a multiple of this value due to the presence of the bridges [Fig. 1(b)], which in the cross sections appear as the big holes close to the surface. It is also important to note how the interconnected porosity increases in the bottom of the

TABLE I. Laser beam characteristics and thickness of the modified layer.

Repetition rate (kHz)	Pulse energy (mJ)	Pulse duration (ns)	Peak irradiance (MW/cm^2)	Mean irradiance (kW/cm^2)	Modified depth (μm)
4	5.1	360	15	21	12
10	3.1	640	5.0	32	20
30	1.2	1100	1.3	38	80
CW	…	…	…	30	80

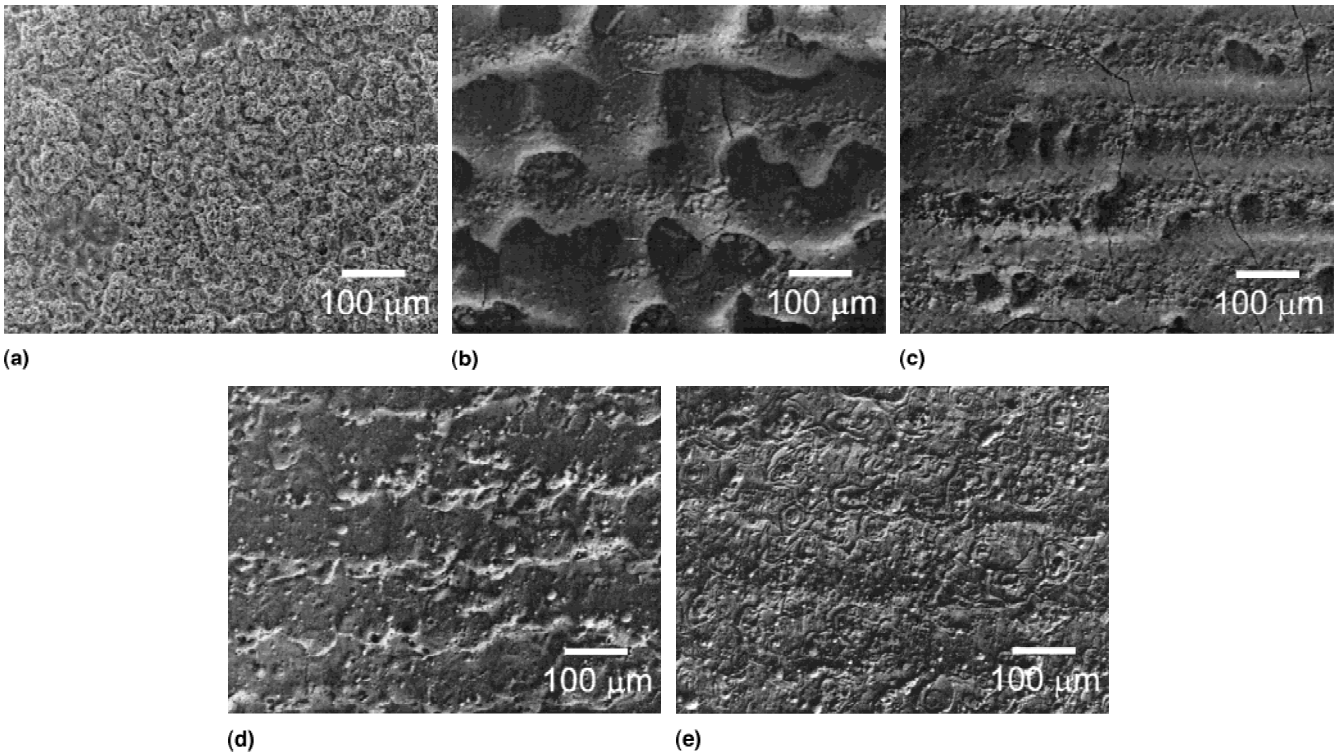

FIG. 1. SEM images of the morphology of the Cr_3C_2–NiCr coatings (a) before laser treatment, and after laser treatment at repetition rates of (b) 4 kHz, (c) 10 kHz, (d) 30 kHz, and (e) in the CW mode.

grooves. It is formed by large pores and can result in the formation of large internal cracks. Figure 2(c) is a cross section of the sample treated at 30 kHz. It reveals the formation of a compact layer in the surface of the coating, about 50 μm deep, without interconnected porosity. Only some large isolated pores appear in the interface between this layer and the bulk of the coating. The image also shows the presence of two thin cracks. It has to be pointed out that an accurate inspection of the whole section reveals that in no case the cracks reach the substrate. Finally, it should also be noted that cross-section images obtained in CW mode are identical to the ones at 30 kHz.

XRD analyses were performed on the untreated sample and on the one treated at 30 kHz (Fig. 3). For the untreated one, several diffraction peaks were identified. They correspond to the crystalline phases of Cr_3C_2, Cr_7C_3, Cr_2O_3, and Ni. In addition, a continuous background is present in the diffractogram. It can be attributed to the formation of amorphous phases during the spraying process.[1] After treatment at 30 kHz, only the peaks corresponding to Cr_7C_3, Cr_2O_3, and Ni appear in the diffractogram. The two peaks at 43.4° and 50.4° can be attributed to Ni alloyed with an important amount of Cr; the alloying would shift the positions of Ni peaks to lower diffraction angles. It was not possible to detect any peak from Cr_3C_2, and the continuous background completely disappeared. The Cr_7C_3 crystalline phase reveals now a strong preferential orientation in the (112) direction.

Figure 4(a) shows a SEM cross section of the untreated sample. It presents several structures imbedded in a matrix. EPMA measurements (Table II) allowed us to determine the nature of the structures. The dark gray, round-shaped grains correspond to Cr_3C_2, the medium gray grains to Cr_7C_3, the black lamellae to Cr_3O_2,[16] and the light gray matrix to the NiCr alloy. These results are in good agreement with XRD measurements. A cross section of the sample treated at 4 kHz is depicted in Fig. 4(b). It clearly shows the grooves previously observed by optical microscopy [Fig. 2(b)] and the large pores and cracks developed in the basis of the walls that surround the grooves. Figure 4(c) presents a cross section of the sample treated at 30 kHz. The morphology in a layer about 80 μm deep in the surface of the coating is completely different from the one deep inside the bulk, identical to the untreated sample. Close to the surface, medium gray, large structures oriented perpendicular to it are imbedded in a light gray matrix. EPMA measurements (Table II) indicate that the medium gray grains correspond to Cr_7C_3, and the light gray matrix to NiCr. It must be pointed out that while the composition of the Cr_7C_3 grains in the modified zone is close to the one in the untreated coating, the NiCr matrix became considerably enriched in Cr. This is in good agreement with the shift of the Ni peaks to low diffraction angles observed in the XRD measurements after laser treatment. The shape of the Cr_7C_3 grains changes to a more irregular and

smaller one at depths of about 50 μm. Deeper inside, at about 80 μm in depth, this morphology evolves to the one of the untreated sample with the presence of the Cr_3O_3 lamellae and the Cr_3C_2 grains. The Cr_2O_3 grains are present in the whole modified zone as dispersed very small black dots whose size begins to increase at depths of about 50 μm until the formation of well-developed lamellae in the unmodified region. The Cr_3C_2 appears at about 70 μm in the form of darker gray grains surrounded by Cr_7C_3. The presence of some isolated pores is also noticeable in the transition zone between the modified layer and the bulk of the coating. This evolution in depth of the structure and composition of the treated coating has been observed at all the repetition rates under study and in the CW mode. Only the thickness of the modified layer varied from one to another. Table I depicts the corresponding values, and it can be observed how they increase monotonically with the repetition rate in the pulsed mode. Once more, the result corresponding to CW mode is practically identical to the one obtained at 30 kHz.

IV. DISCUSSION

The differences observed in the treated coatings at the different laser repetition rates arise from the fact that energy was delivered to the material in a different way for each one. As mentioned above, the heating process can be analyzed through inspection of the values of peak and mean laser irradiances. Since in this study the values of the mean irradiances are quite similar for all the laser repetition rates in comparison to the strong differences between peak irradiances (Table I), it can be stated that the higher the peak irradiance, the faster the heating rate. In terms of laser parameters, the lower the repetition rate, the faster the heating rate.

The images corresponding to the treated samples in Fig. 1 reveal that melting occurred under irradiation at all the studied repetition rates, a necessary condition for achieving the required sealing effect. However, at low repetition rates [Figs. 1(b) and 1(c)], the surface is not only molten, but also an important amount of material was removed from the coating, as is evidenced by the presence of the deep grooves [Figs. 1(b), 1(c), 2(b), and 3(b)]. They are formed by the most intense central part of the beam (about 100 μm diameter) as it scans the surface of the sample. Efficient material removal requires fast heating while slow heating is needed to melt without

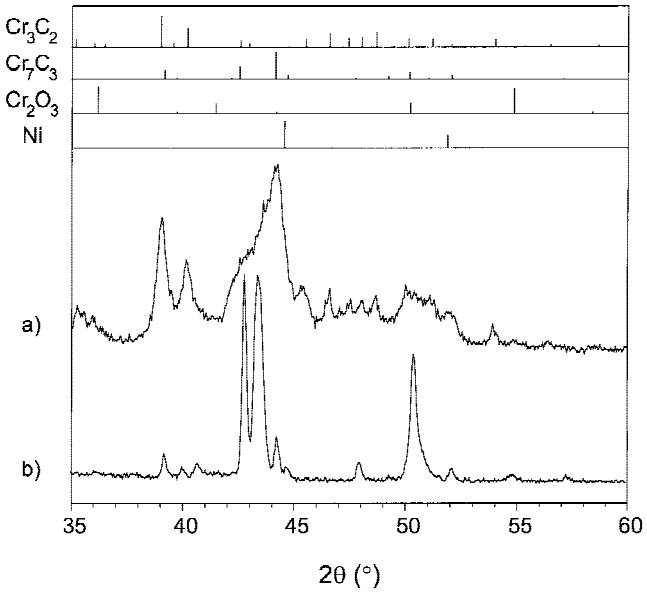

FIG. 3. XRD diffractograms of the Cr_3C_2–NiCr coatings (a) as-sprayed and (b) after laser treatment at 30 kHz. The patterns of the crystalline phases present in the diffractograms are also included. Ni peaks are shifted to low angles when alloyed with Cr.

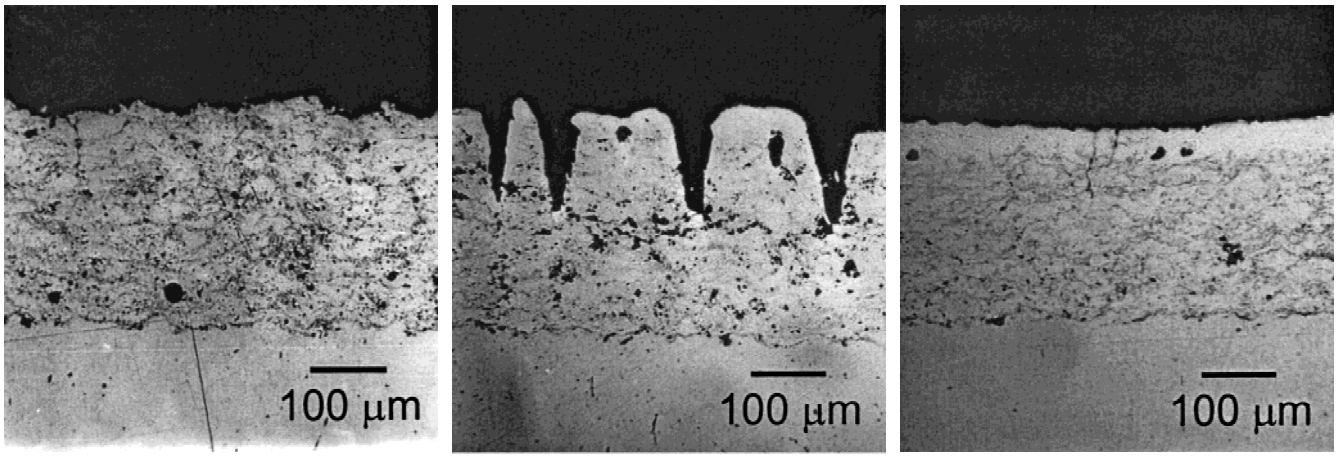

FIG. 2. Optical microscopy cross sections of the Cr_3C_2–NiCr coatings (a) before laser treatment, and after laser treatment at repetition rates of (b) 4 kHz and (c) 30 kHz.

strong vaporization, which accounts for the formation of the grooves at 4 and 10 kHz and the only molten aspect of the morphologies obtained at 30 kHz and in the CW mode. The differences between peak irradiances depicted in Table I can also explain the presence of an extensive crack network at 4 and 10 kHz since fast and localized thermal changes promote their formation. Otherwise, at 30 kHz and at CW mode, where heating and cooling rates are slower, cracks are occasional and shallow. Regarding the small holes, droplets and bubbles present at 30 kHz and at CW mode can be attributed to the release of entrapped gas during melting.[9,10,15,17] The slow heating process allows bubbles to coalesce and escape leaving small holes and droplets on the surface. At low repetition rates, the heating rate is high, and in addition, the thickness of molten material is small (Table I), so that bubbles do not have time to coalesce.[17] This could explain the absence of these structures at 4 and 10 kHz. One important consequence of the slow heating rates is that thicker modified layers can be obtained (Table I). As shown in Fig. 2(c), the modified layer is perfectly compact, and therefore, it is completely sealed. Thus the thicker the modified layer, the more efficient the sealing effect. Summarizing, it is clear that the best laser surface treatments were achieved at high repetition rates or in

TABLE II. Chemical composition of the untreated and the laser-treated samples determined by EPMA.

	Composition, at.%					
	Untreated sample			Laser treated sample		
Material	C	Cr	Ni	C	Cr	Ni
Cr_3C_2	40	60	1	…	…	…
Cr_7C_3	30	66	7	34	60	5
Ni (Cr,C)	3	23	74	12	44	43

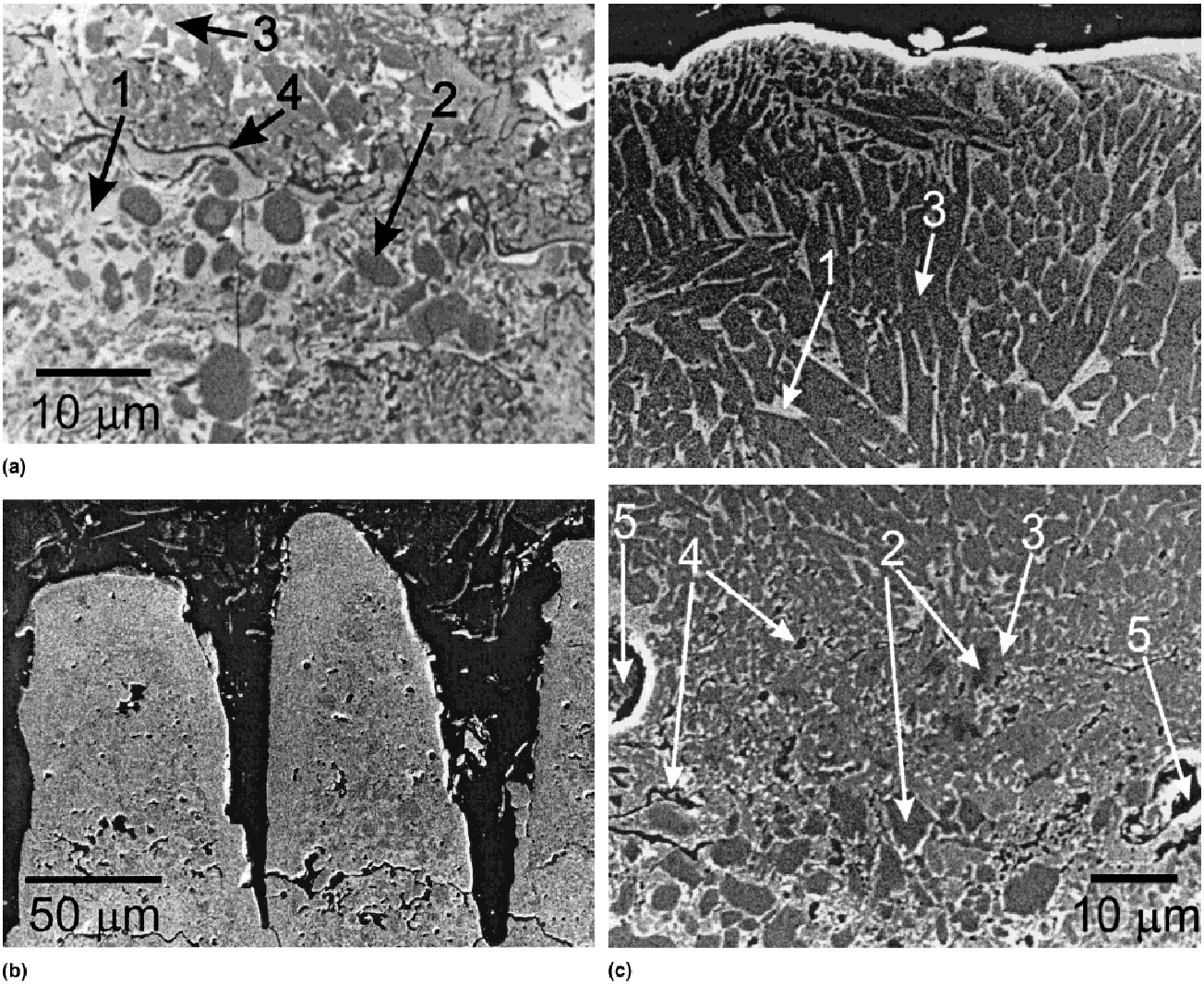

FIG. 4. SEM cross sections of the Cr_3C_2–NiCr coatings (a) before laser treatment, and after laser treatment at repetition rates of (b) 4 kHz and (c) 30 kHz. Numeric labels correspond to (1) NiCr, (2) Cr_3C_2, (3) Cr_7C_3, (4) Cr_2O_3, and (5) pores.

CW mode. At low repetition rates, the presence of grooves and extensive cracks would be detrimental in corrosion and wear resistance applications. Because of that, the compositional analysis was only carried out for the sample with good sealing obtained at 30 kHz laser repetition rate.

From the XRD, SEM cross-sections, and EPMA results presented above for this sample it is possible to explain the composition and phases distribution of the thick modified layer in the surface of the coating. Under the action of the laser beam, the material temperature is raised up at the same time that heat propagates deep inside the coating. When the temperature reaches the NiCr melting point it becomes liquid and dissolves the carbides and oxides. The dissolution of these compounds will only be complete if the solvent persists enough time in the liquid state. If the temperature reaches their respective melting points before complete dissolution, the compounds would directly melt. When the action of the laser beam ceases, the melt pool cools down and solid ceramic phases are formed, a process that lasts until the solvent (NiCr) completely solidifies. This leads to the massive formation of Cr_7C_3 [Fig. 4(c)], in spite of the other initial ceramic phases (Cr_3C_2 and Cr_2O_3). The total absence of Cr_3C_2 in the modified zone indicates that formation of Cr_7C_3 is the most efficient process under the fast cooling conditions of the laser treatment, in contrast to the equilibrium case, where Cr_3C_2 would form. Regarding the oxide, it seems that, although the treatment is carried out in air, there is no important oxidation of the material. There are some very small Cr_2O_3 grains in the modified layer, but it is evident from comparison between it and the unmodified zone [Fig. 4(c)] that the presence of the oxide is much lower in the former region. The decrease in the Cr_2O_3 content after treatment is an important achievement, since the presence of this oxide is detrimental for the mechanical and chemical properties of the coating.[16] The enrichment in Cr and C in the NiCr matrix observed after treatment (Table II) could be due to the solidification of the metal prior to the complete carbon exhaustion during the formation of the ceramic compounds. The absence of a continuous background in the XRD analyses indicates that the processes described above, although fast, are not fast enough to produce amorphous phases as occur during spraying.[1,3]

Once all of these considerations are taken into account, it is possible to explain the phases distribution in the modified layer by inspection of the heat flow rates during cooling. The melt pool produced during the action of the laser beam cools down mainly through the outer surface of the sample and through the bulk of the coating, in the bottom of the pool. The main direction of cooling is normal to the sample surface. Close to it, the cooling rate is high and, therefore, solidification will lead to the formation of small Cr_7C_3 grains, as it corresponds to fast crystallization processes. Figure 4(c) indeed displays an approximately 7-μm-deep layer formed of small grains (between 1 and 5 μm) oriented along the cooling direction. Deeper inside the material, at depths between 10 and 50 μm, the size of the grains increases to values up to 25 μm and their shapes become elongated [Fig. 4(c)]. In the inner parts of the melt pool the cooling rates are much slower than in the frontier and allow big grains to crystallize. The presence of big ceramic grains can enhance the wear resistance properties of the coating, especially when abrasive wear mechanisms are involved.[18] As in the previous case, they show a main orientation along the cooling direction. This anisotropy imposed by cooling processes is possibly responsible for the preferential orientation of the (112) crystalline direction observed in XRD analyses. Finally, in the bottom of the pool [transition zone between 50 and 80 μm in Fig. 4(c)] the temperature is lower than in the inner parts, and in addition, cooling rates are extremely fast, since the bottom of the pool is in good thermal contact to the bulk of the coating, which presents an important metallic content. This makes the melt solidify before complete dissolution of Cr_3C_2 and Cr_2O_3, as is indicated by the presence of residual Cr_3C_2 grains surrounded by crystallized Cr_7C_3 and partially dissolved Cr_2O_3 lamellae [see Fig. 4(c)]. As a consequence, the Cr_7C_3 grains are very small (about 1 μm) and oriented quite at random. The presence of large isolated pores in the transition region [Figs. 2(c) and 3(c)] can also be explained according to the thermal history of the modified zone following the action of the laser: the bottom of the melt pool persists long enough in the liquid state for bubbles to nucleate, but before they can leave this region, the material solidifies quickly and they remain trapped in their positions. Upper layers do not show pores since the melt lasts so long that bubbles can escape, and thus develop the structures observed in the surface of the samples in Figs. 1(d) and 1(e).

V. CONCLUSION

The laser surface treatment of Cr_3C_2–NiCr coatings at low repetition rates, which have associated high peak irradiances, produces surface morphologies with deep grooves along the laser tracks and many cracks. Disregarding the deep grooves, the laser-modified superficial layer is very shallow.

At high repetition rates and in the CW mode, that is, at low peak irradiances, the sample surface presents an aspect that evidences melting and resolidification processes. No grooves have been detected and only some superficial cracks are present; in no case do they reach the substrate. In both cases the laser beam modifies a superficial layer of about 80 μm (25% of the coating thickness), which is mainly formed from large Cr_7C_3

grains embedded in a metallic NiCr matrix. The oxide content of this layer is considerably lower than that of the untreated coating. The formation of these big ceramic grains in the surface zone could be beneficial for corrosion and wear resistance applications.

In summary, the optima laser surface treatments of Cr_3C_2–NiCr coatings for corrosion and wear resistance applications must be carried out in those conditions corresponding to low peak irradiances. High peak irradiances led to the formation of a great amount of defects, which are clearly detrimental for the desired applications.

ACKNOWLEDGMENTS

This work is part of a research program financed by Ministerio de Ciencia y Tecnología (MCYT) of the Spanish Government (MAT98-0334-C02-01) and Departament d'Universitats, Recerca; Societat de la Informació (DURSI) of the Catalan Government (1999SGR00056 and 1999SGR00051).

REFERENCES

1. J.M. Guilemany, J. Nutting, and N. Llorca-Isern, J. Therm. Spray Technol. **5,** 483 (1996).
2. J. Li, Y. Zhang, J. Huang, and C. Ding, J. Therm. Spray Technol. **7,** 242 (1998).
3. B. Wang, in *Proceedings of the 11th International Conference on Surface Modification Technologies*, edited by T.S. Sudarshan, M. Jeandin, and K.A. Khor (The Institute of Materials, London, United Kingdom, 1998), p. 458.
4. F. Otsubo, H. Era, T. Uchida, and K. Kishitake, J. Therm. Spray Technol. **9,** 499 (2000).
5. J. He, M. Ice, and E.J. Lavernia, Metall. Mater. Trans. A **31,** 555 (2000).
6. J. He and E.J. Lavernia, Mater. Sci. Eng. A **301,** 69 (2001).
7. P. Serra, J.M. Miguel, J.L. Morenza, and J.M. Guilemany, in *Laser Materials Processing*, Vol. 89 (Laser Institute of America, Orlando, FL, 2000), p. 194.
8. S.C. Tjong, Thin Solid Films **274,** 95 (1996).
9. J. Mateos, J.M. Cuetos, E. Fernández, and R. Vijande, Wear **239,** 274 (2000).
10. Y. Fu, A.W. Batchelor, H. Xing, and Y. Gu, Wear **210,** 157 (1997).
11. G.Y. Liang and T.T. Wong, Surf. Coat. Technol. **89,** 121 (1997).
12. H.C. Chen, E. Pfender, and J. Heberlein, Thin Solid Films **315,** 159 (1998).
13. L. Pawlowski, J. Therm. Spray Technol. **8,** 279 (1999).
14. S. Tondu, T. Schnick, L. Pawlowski, B. Vielage, S. Steinhäuser, and L. Sabatier, Surf. Coat. Technol. **123,** 247 (2000).
15. K.A. Khor, A. Vreeling, Z.L. Dong, and P. Cheang, Mater. Sci. Eng. A **266,** 1 (1999).
16. J.M. Guilemany and J.A. Calero, in *Proceedings of the 11th International Conference on Surface Modification Technologies*, edited by T.S. Sudarshan, M. Jeandin, and K.A. Khor (The Institute of Materials, London, United Kingdom, 1998), p. 81.
17. K.C. Chang, W.J. Wei, and C. Chen, Surf. Coat. Technol. **102,** 197 (1998).
18. H. Wang, W. Xia, and Y. Jin, Wear **195,** 47 (1996).